

RFID Techniques for Passive Electronics

Senior Project

**By
Ryan Behr
David Cobos**

Electrical Engineering Department
California Polytechnic State University
San Luis Obispo
2011

Table of Contents

Section	Page
List of Tables and Figures.....	IV
Acknowledgements.....	VI
I. Introduction.....	7
II. Background.....	8
III. Requirements.....	10
IV. Design.....	11
4.1 Theory of Operation.....	11
4.2 Inductors.....	14
4.3 Circuit Design.....	15
V. Development and Construction.....	24
VI. Integration and Testing.....	29
VII. Conclusion and Recommendations.....	33
VIII. Bibliography.....	35

Appendices

A. Parts Lists and Costs.....	36
B. Time Allocation Estimates.....	36
C. Derivation of Operating Principle.....	37
D. Picture of Prototype.....	40

List of Tables and Figures

Tables

	Page
1. Parts List and Cost.....	36
2. Schedule – Time Estimates.....	36

Figures

1. Schematic of Magnetically Coupled Inductors with Split Supply Rectification.....	11
2. Pot Core.....	15
3. Coil Wire and Pot Core.....	15
4. Insufficient V _{ee} Voltage with NMOS Substrate Internally Grounded.....	18
5. Full Schematic of Final Circuit.....	20
6. Supply Voltages Across Split Supply Capacitors.....	20
7. Modulating Signal on Primary Coil.....	21
8. Output of Envelope Detector.....	21
9. Output of Low-pass Filter.....	22
10. Output of Amplification Stage.....	22
11. Screenshot of Inductance Calculator Used.....	24
12. Smith Chart Plot of 1.81 μ H Primary Inductor.....	26

13.Smith Chart Plot of $6.197\mu\text{H}$ Secondary Inductor.....	27
14.Primary (Left) and Secondary (Right) Inductors Used in Final Circuit.....	27
15.Channel 1 (Top) Signal Across Primary Inductor; Channel 2 (Bottom) Voltage Across VCO.....	29
16.Channel 1 (Top) Showing the Output of the VCO; Channel 2 (Bottom) Showing the Output of Low-pass Filter.....	31
17.Channel 1 (Top) Showing the Output of the VCO; Channel 2 (Bottom) Showing the Output of the Amplification Stage.....	31
18.An Equivalent T Circuit with an Open Load.....	37
19.An Equivalent T Circuit with a Short Load.....	38
20.Picture of Prototype.....	40

Acknowledgements

We would like to thank Dr. Prodanov for his endless patience and assistance throughout the duration of this project.

I. Introduction

Magnetic coupling refers to a phenomenon that results when two conductors are arranged in such a way, such that, when electric current flowing through one of the conductors changes it results in an induced voltage on the other conductor via the magnetic field produced by the current changing conductor. The coupling between two wires can be increased by winding them into coils and placing them close together on a common axis, so the magnetic field of one coil passes through the other coil. This phenomenon is a product of electromagnetic induction, in which, as explained by Faraday's Law, a time-varying current in one coil produces a time-varying magnetic field which produce currents in the receiving coil. In actuality, the time-varying magnetic field produces an electric field that circulates around the time-varying magnetic field. It is this induced electric field that applies a force on the free electrons in the receiving coil, thus generating electric current. This principle forms the basis of a seemingly infinite array of applications within the field of electrical engineering, and specifically as it pertains to this project, wireless energy transfer and data transmission.

II. Background

The goal of this project is to implement a wireless system which is capable of wirelessly transferring power to, and receiving data from a passive electronic sensor. More specifically, to design and test a circuit that will wirelessly harvest power for circuit operation and transmit sensor data back to the power source for signal readout. The type of sensor to be used will be a passive digital tire pressure sensor. The sensor must be small in physical size and capable of being inserted on the inner wall of a vehicle tire. A passive device is one without a battery or an external power supply. LT Spice will be used as a simulation tool in devising and optimizing a circuit capable of this type of communication. The circuit will utilize magnetically coupled coils that function as antennae to supply power as well as transmit data. The primary, or source coil, will be connected to a signal generator that generates an alternating current. The secondary coil will be connected in a circuit topology using two diodes with opposing polarity, and two capacitors to rectify the alternating signal into two DC voltages. The fundamental principle that this circuit relies on for operation is the ability to change the impedance seen by the signal generator on the primary side, this is accomplished by “open” and “short”

circuiting the secondary coil. A switch will be placed across the terminals of the secondary coil, and the state of the switch, whether it is open or closed, will determine the impedance to the signal generator on the primary side by modulating the magnetic field of the coupled coils. Varying the impedance seen by the source effectively modulates the signal on the primary coil. The voltage across the primary coil should switch between two levels, the different voltage levels can be used as different logic levels, and binary data can be obtained. Implicit in this theory is the sensor output must be digital data, as opposed to an analog signal, and the digital output must be capable of toggling the switch across the secondary coil. The binary data obtained from the primary coil can be interpreted and readout in any desired fashion.

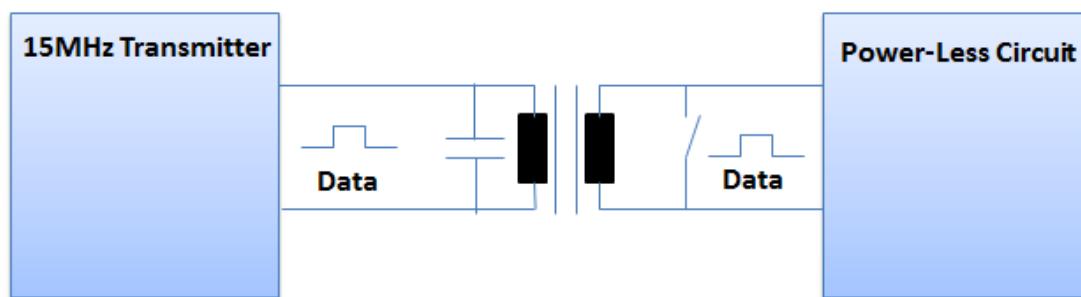


Figure 1: System Block Diagram

III. Requirements

The end goal of this project is to design and test a circuit that will operate at 15MHz and wirelessly harvest power for a digital tire pressure sensor, and transmit sensor data back to the power source for pressure data readout. In order to accomplish such an undertaking the following objectives must be met:

1. Design, construct, and characterize coils to function as antennae at 15MHz
2. Construct a full-wave rectifier to be used in a split supply fashion
3. Generate a clock signal on the secondary side to operate the sensor and transmit data at a chosen low frequency in the kilohertz range
4. Implement a bilateral switch to open and short the secondary coil
5. Connect an envelope detector circuit to the primary coil to obtain the amplitude modulated signal from the 15MHz carrier signal

IV. Design

4.1 Theory of Operation

By placing two inductors in close proximity on a common axis a constant frequency can be transmitted from the primary side inductor to the sensor side inductor. Inserting two diodes in parallel with opposing polarity and adding a capacitor in series with each diode creates two DC voltage rails which can be used to supply power to the sensor network. To maximize the voltage difference across the rails a split supply is used, this means one rail is positive and the other negative with respect to ground. Figure 2 below can be used to gain an intuition of the proposed operation.

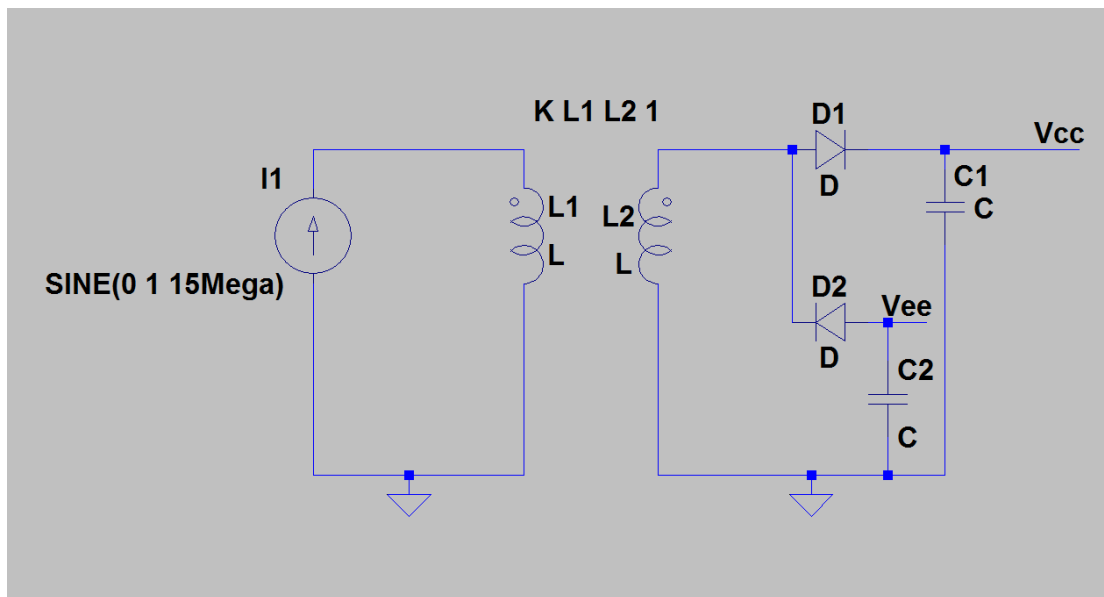


Figure 2: Schematic of Magnetically Coupled Inductors with Split Supply Rectification

In reference to Figure 2, using near-field coupling the alternating current supplied to the primary coil is transmitted to the secondary coil. V_{cc} would have 2.5V positive with respect to the reference ground voltage, and V_{ee} would have 2.5V negative with respect to the reference ground voltage. So the voltage difference across terminals V_{cc} and V_{ee} is 5V and it would be used to supply power to the digital sensor part number MPL115A1.

The driving source of the primary coil operates at a frequency of 15MHz. This frequency was selected for multiple reasons. This particular frequency lies within the industrial, scientific, and medical (ISM) radio band, an internationally reserved frequency range for industrial, scientific, and medical purposes other than communications. Additionally, system functionality relies on the ability to induce a voltage in the secondary coil via the primary inductor. The voltage across the primary inductor, V_1 , and the voltage induced across the secondary inductor, V_2 , is given by the following relations:

$$V_1 = \omega L_1 I_1 \cos(\omega t + 90^\circ) \quad (1)$$

$$V_2 = \omega k \sqrt{L_1 L_2} I_1 \cos(\omega t + 90^\circ) \quad (2)$$

where k is the coupling coefficient between the two inductors, ω is the angular frequency of the system, I_1 is the magnitude of the current in the primary inductor, and L_1 and L_2 are the inductor values in Henries. What is to be derived from the above equations is the fact that V_2 increases as the frequency increases, so using the relatively high frequency of 15MHz is imperative in being able to meet voltage

demands across the secondary coil, while not requiring excessive voltage and current in the primary inductor.

Not shown in Figure 2 is a switch placed across the terminals of the secondary coil. The function of the switch is to change the impedance seen by the driving source on the primary side. Changing the load presented to the primary side requires L_2 to vary. L_2 is effectively short circuited when the switch is closed, resulting in a different inductance seen at the primary side, which will be called L_{seen} . When small current is drawn from the capacitors, little current is drawn through the diodes, and L_2 is effectively open circuited. The state of the switch, open or closed, will be determined by the output of the sensor, and since the sensor outputs digital data the varying load will fluctuate between two distinct levels. The inductance seen at the primary side, L_{seen} , is expressed in the following equations:

$$\text{secondary is open circuited: } L_{seen} = L_1 \quad (3)$$

$$\text{secondary is short circuited: } L_{seen} = L_1(1-k^2) \quad (4)$$

where again k is the coupling coefficient between the two coils. It is important to note that short circuiting the secondary coil does not discharge the capacitors, the charge on the capacitors is held captive due to the diodes being reversed biased, short circuiting only changes the impedance seen by the driving source. Varying the impedance presented to the signal generator on the primary side modulates the voltage presented to the primary coil. Modulation on the primary inductor enables the digital sensor data to be measured.

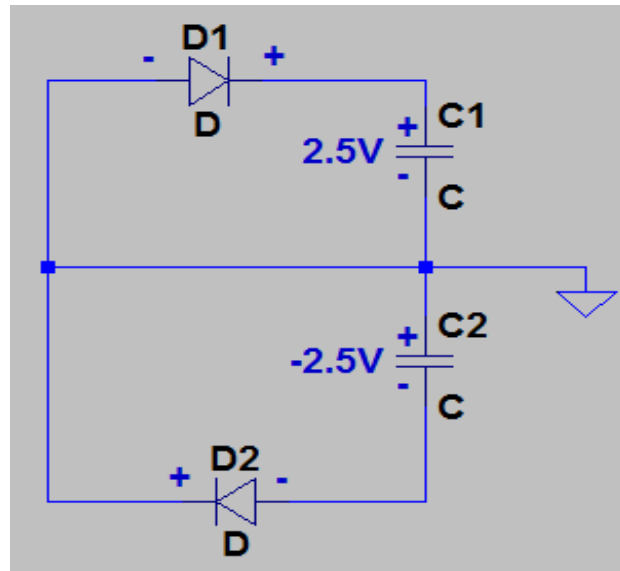


Figure 3: Secondary circuit when switch is ON

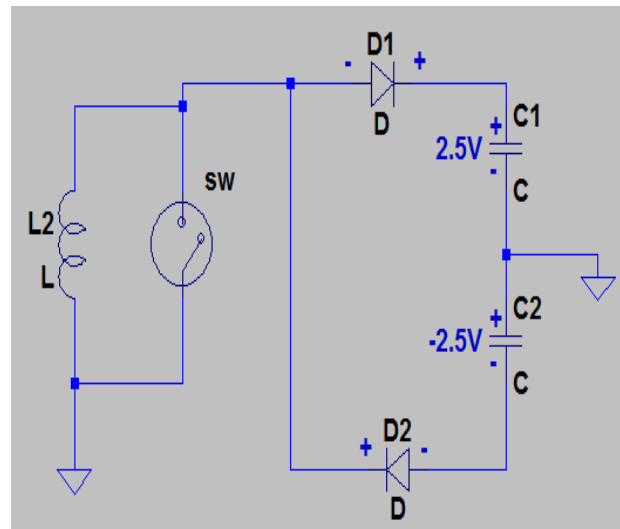
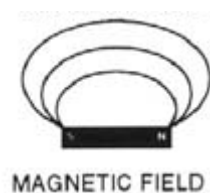


Figure 4: Secondary circuit when switch is OFF

4.2 Inductors

In an effort to reduce the overall size of the passive sensor the inductors must be very small. Designing an inductor to function as an antenna eliminates toroid cores from being used. For this application pot core inductors are ideal. A pot core, pictured below in Figure 6, is round with an internal hollow that almost completely encloses the coil. In the center of the hollow is a bobbin which the coils are formed around. The advantage of a pot core is the shielding effect provided by the outer rim which acts to prevent radiation and electromagnetic interference. Furthermore, the magnetic flux radiates solely in one direction due to the flux lines forming closed loops around the bobbin and outer wall. This virtually eliminates losses due to leakage flux and optimizes energy transfer. The wire used for winding the coils, shown in Figure 7, is 30-gauge enamel-covered solid-conductor copper wire purchased at RadioShack. The inductors should have a reactance of 100 – 1000 Ohms at the operating frequency. After construction the values are to be verified.



**Figure 5: Magnetic Shielding, most of magnetic radiation occurs in one direction
allowing stronger coil coupling**



Figure 6: Pot Core

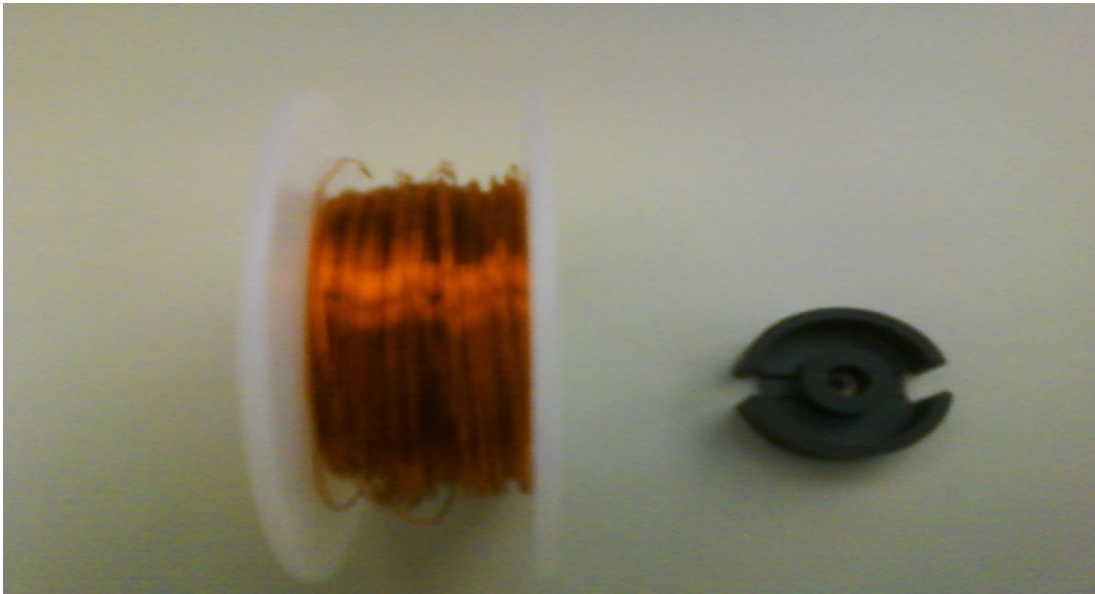


Figure 7: Coil Wire and Pot Core

4.3 Circuit Design

The system requires two coils in the micro Henry range with a reactance of 100 – 1000 Ohms at 15MHz. The coils must have low parasitic capacitance and be capable of operating as an “inductor” at this frequency. As more wire is coiled in an

effort to increase inductance large parasitic capacitances are created due to charge separation along the coils, this implies that there exists a natural bound maximum inductance that can be created in practice and used at 15MHz. A self-resonance frequency exists for all inductors in which an inductor takes on enough capacitive tendencies that it cancels out the inductive tendencies, thus rendering the device useless as an inductor. Precaution must be taken to avoid creating inductors that have a self-resonance frequency near 15MHz. Verification of the inductors is necessary to select an appropriate capacitor to be placed in parallel on the primary side (see figure 8). Capacitor selection is based on creating a parallel LC resonance circuit. A parallel resonant circuit provides current magnification, which reduces the amount of current required from the function generator to drive the circuit. Accurate measurement of the inductors allows the following equation to be rearranged, and the value of C to be solved for:

$$\text{resonant frequency: } f = \frac{1}{2\pi\sqrt{LC}} \quad (5)$$

The desired resonant frequency is the operation frequency of the system, which is 15MHz.

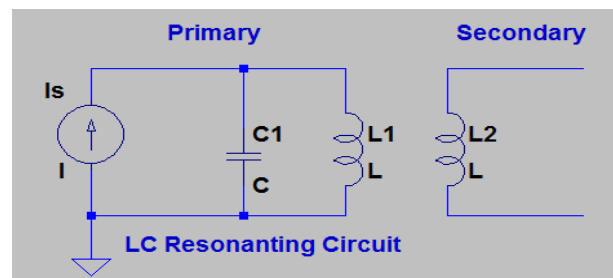


Figure 8: LC resonating circuit used to increase current injection from source

Component selection is crucial for operation, in particular selection of the diodes. Many rectifying diodes exist but are typically rated for higher voltages and currents and bring in substantial capacitances making them undesirable for RF applications. The diodes must be small in size to reduce capacitance as well as have low forward voltage drop. The forward voltage drop should be in the range of 0.2 – 0.3V. For this surface mount RF Schottky barrier diodes were chosen (part number HSMS-2822).

Varying the load of L_2 means that it must have a load that can act quickly as a short or an open. A switch placed across the terminals of the coils is required. Most MOSFETs on the market have an internally connected substrate; however, this application requires a substrate capable of being connected externally. The reason for this is due to the split supply configuration, where the reference ground voltage is no longer the lowest potential. The substrate must be tied to the lowest potential, and in this case it is the negative capacitor of the split supply, which has a negative voltage with respect to ground. Initially sensor data was output to a CMOS analog switch, which was used to control an NMOS transistor with an internally connected substrate placed across the secondary inductor. This resulted in an asymmetric build up of the supply voltages, as depicted below in Figure 9, where V_{cc} was unaffected but the capacitor responsible for V_{ee} was never able to charge due to the transistor being forced into saturation without a properly connected substrate.

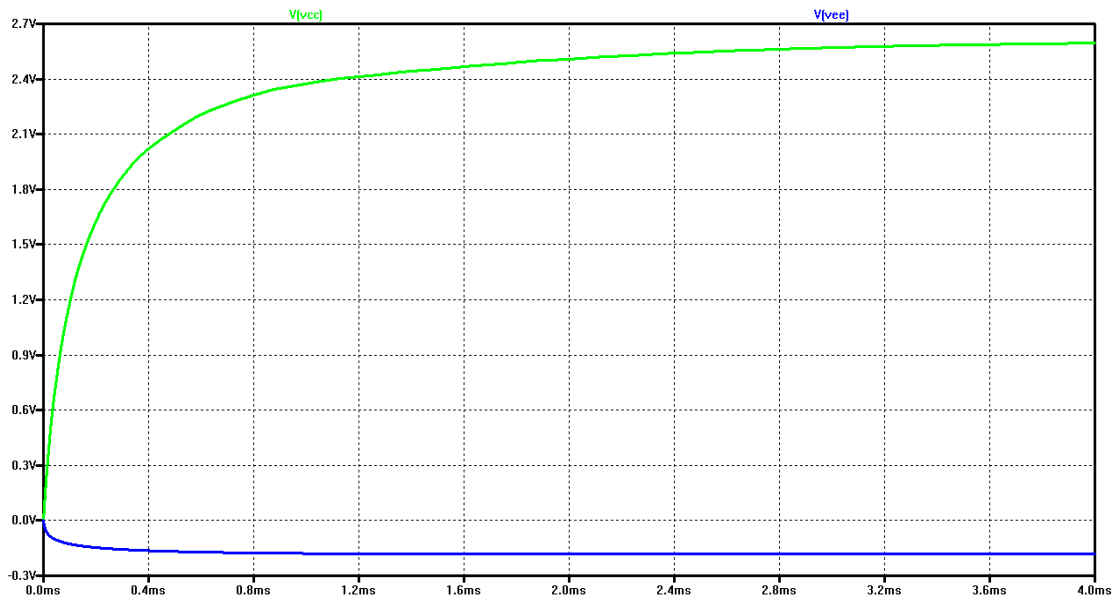


Figure 9: Insufficient V_{ee} Voltage with NMOS Substrate Internally Grounded

A bilateral switch was then selected with separate access to substrate and V_{DD} .

Connecting V_{DD} to the positive capacitor and the substrate to the negative capacitor creates a symmetric circuit and insures equal voltage difference between V_{CC} and ground, and ground and V_{ee} , and thus enabling the split supply to provide adequate voltage for the sensor. The control pin of the switch is connected to the output of the sensor. The digital data of the sensor toggles the switch, shorting L_2 when the output is high and opening L_2 when the output is null. The bidirectional nature of the switch allows either end of the switch to be connected to either end of the inductor.

In order to obtain data from the primary coil an envelope detector circuit must be used. An envelope detector contains a diode, capacitor, and resistor and acts to rectify the 15MHz carrier frequency leaving only the positive modulating

envelope frequency. A similar type of Schottky diode will be used and the resistor and capacitor value will be selected based on the relation:

$$f_c > \frac{1}{2\pi RC} \quad (6)$$

where f_c is the 15MHz carrier frequency. Either the resistor or the capacitor value can be selected and the other solved for. A 10pF capacitor was chosen and a 1k Ω resistor was calculated.

The output of the envelope detector is fed into a low-pass filter consisting of a resistor and a capacitor. The low-pass filter acts to remove the 15MHz carrier frequency leaving only the modulating envelope frequency, which is in the low kilohertz range. The selection of the resistor and capacitor value is determined by the relation:

$$f = \frac{1}{2\pi RC} \quad (7)$$

where f is the frequency of the data, and R and C are the values of the resistor and capacitor in ohms and farads respectively. A 10nF capacitor was selected and a 4k Ω resistor was calculated.

The clean signal from the low-pass filter can then be amplified for use with a microcontroller.

The complete circuit schematic as well as corresponding waveforms from various stages are depicted in the following figures.

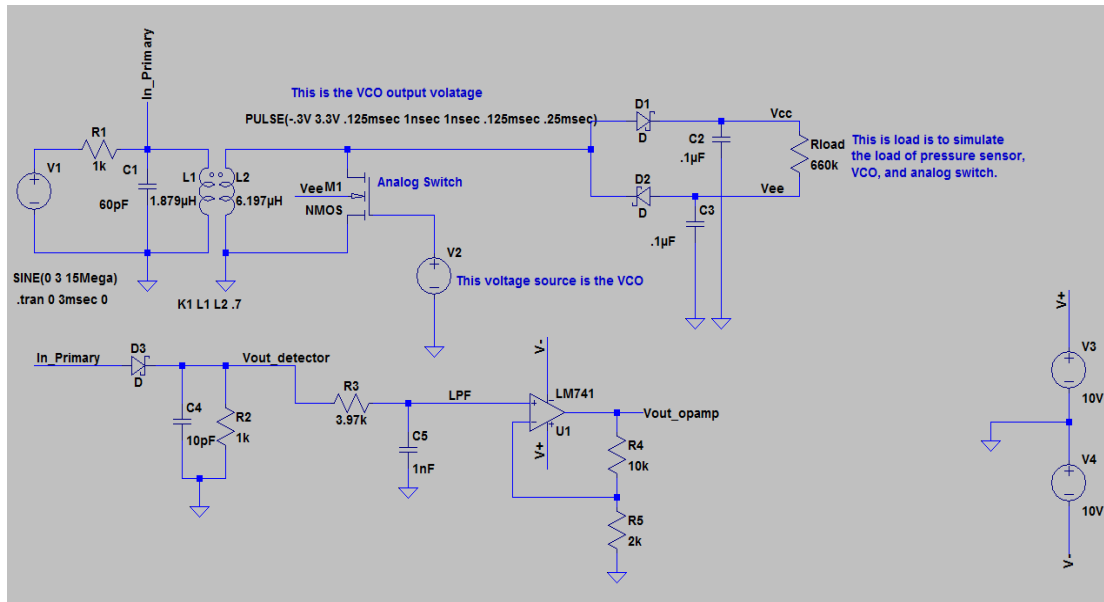


Figure 10: Full Schematic of Final Circuit

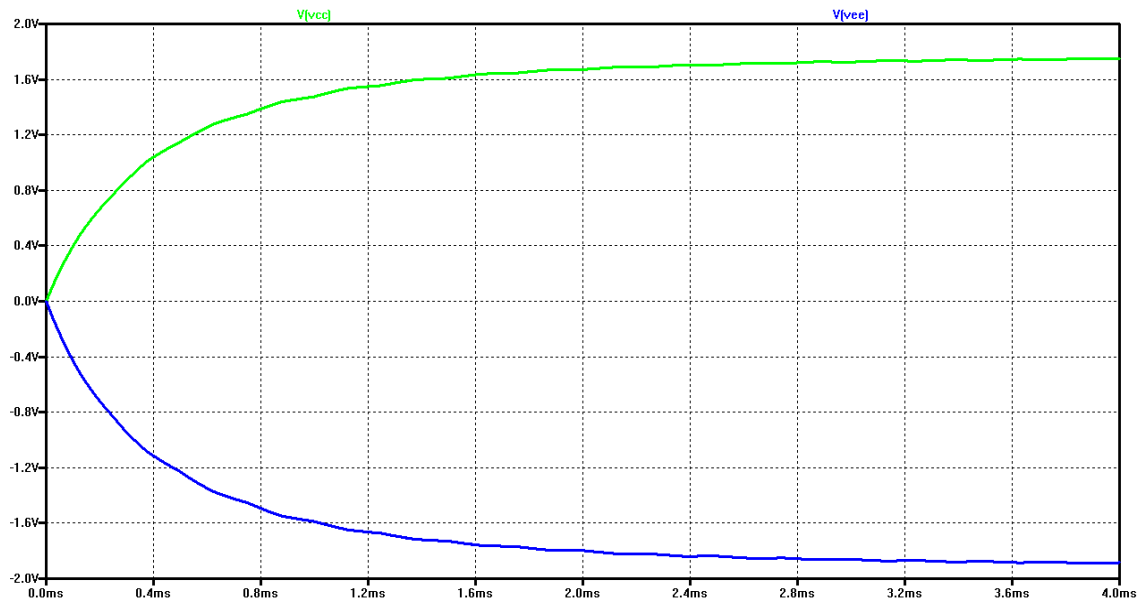


Figure 11: Supply Voltages Across Split Supply Capacitors

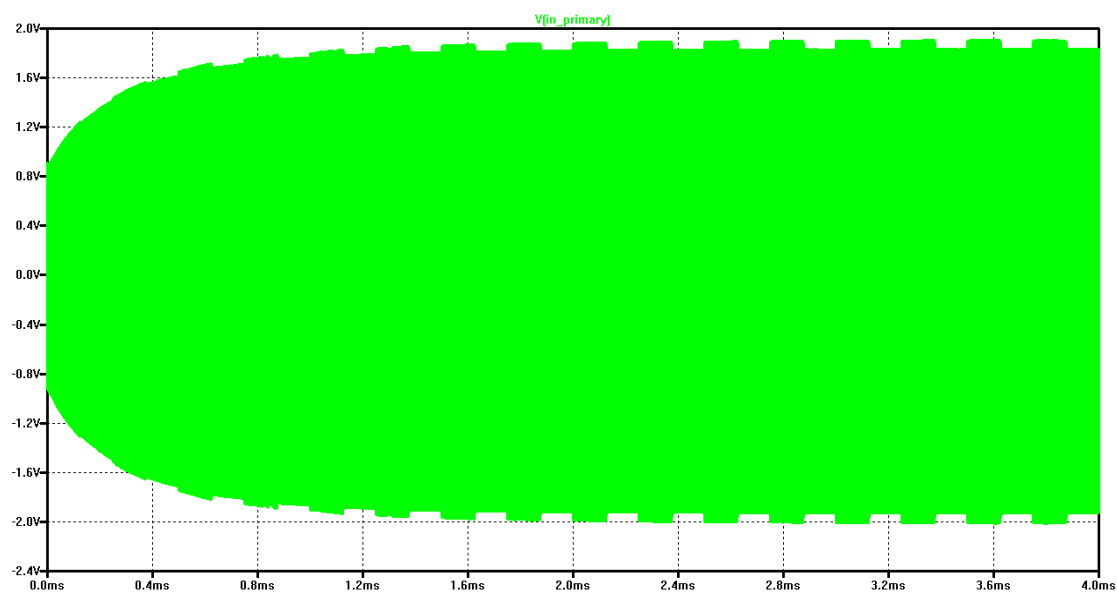


Figure 12: Modulating Signal on Primary Coil

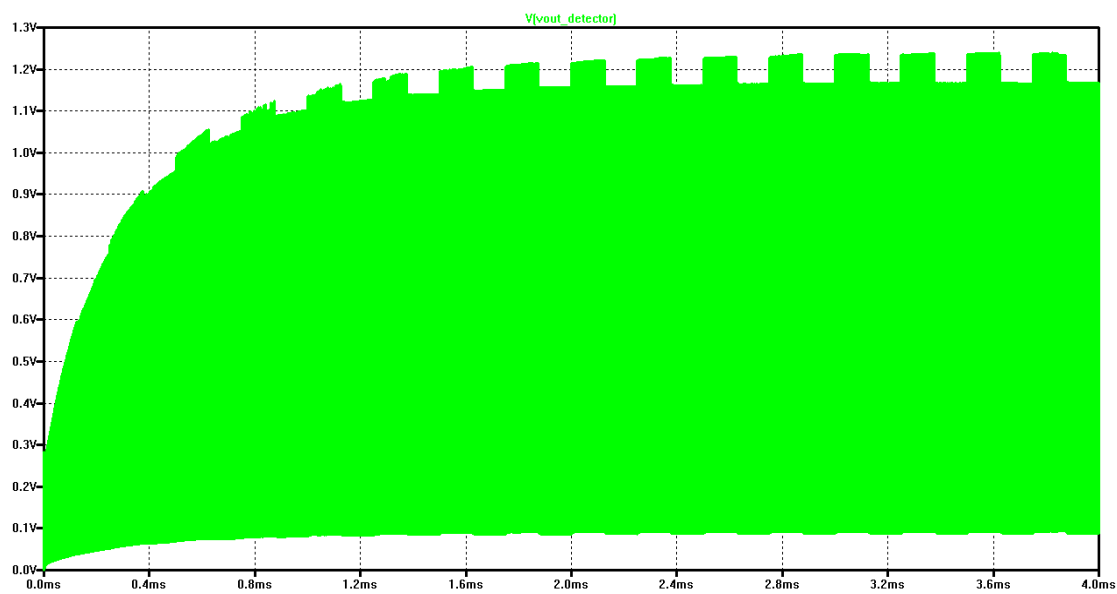


Figure 13: Output of Envelope Detector

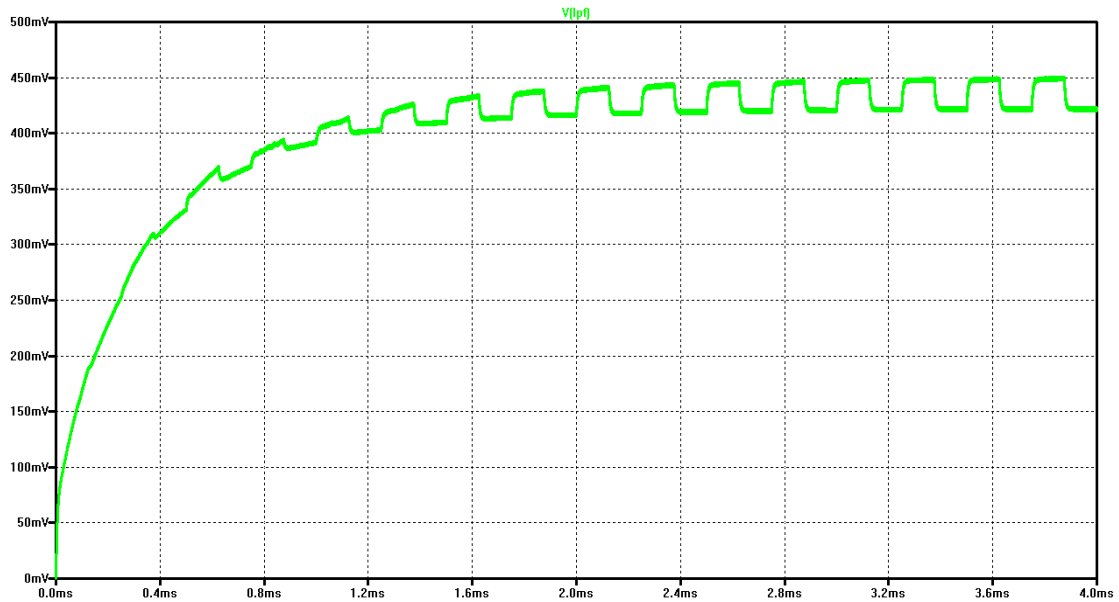


Figure 14: Output of Low-pass Filter

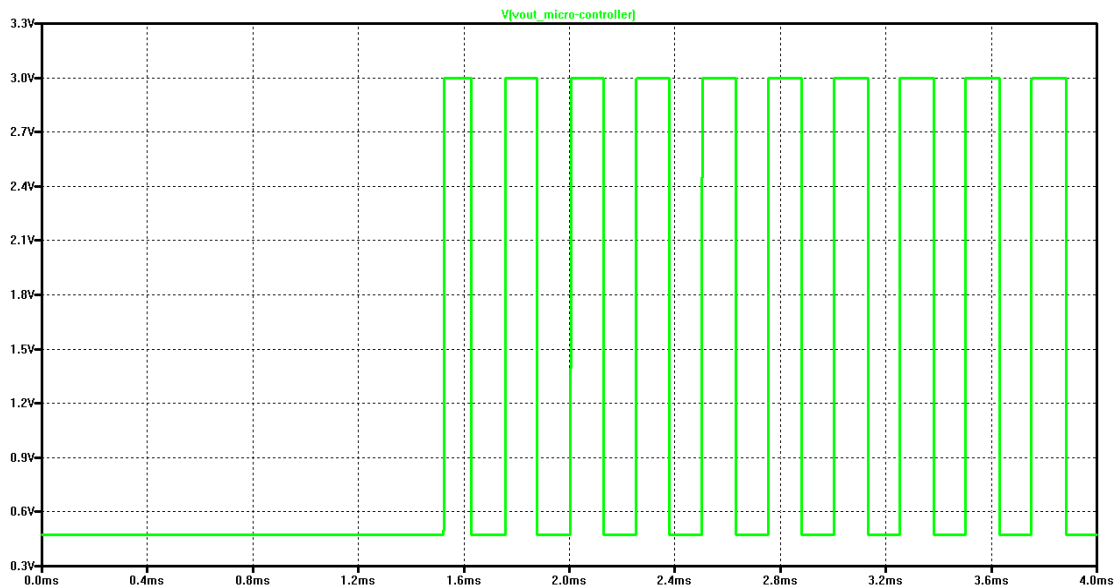


Figure 15: Output of Amplification Stage

Figure 10 represents the final circuit to be implemented. The buildup of supply voltage across the split supply rectifier is represented in Figure 11, where symmetry can now be seen. The different output stages are shown in Figures 12, 13, 14, and 15. The final amplification stage consists of a non-inverting operational amplifier.

The level of amplification was chosen on the basis of achieving greater than 1V peak, which most microcontrollers will accept as logic high. The level of amplification can be adjusted as needed by adjusting the resistors of the non-inverting topology.

V. Development and Construction

The first step in the build process was the assembly of the inductors. Initially a scientific design approach was taken with the use of an inductance calculator. The inductance calculator, shown in Figure 16, takes into consideration the number of turns, the magnetic permeability of the core, the wire radius, and the radius of the core and uses an equation to determine an inductor value.

Inductance Calculations: Circular Loop

[Custom Coils](#) Air Wounds and Toroids Tunable Coils [emiconcorp.com](#)

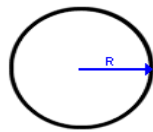
[Digi-Key - High Quality](#) Components & Superior Service - Find Thousands of Products Today! [www.digikey.com](#)

[Hook-Up Wire](#) UL & Military approved. In stock. RoHS compliant. All colors. [www.WeicoWire.com](#)



Ads by Google

Loop of wire with circular shape



N	<input type="text"/>	[]	number of turns
R	<input type="text"/>	[m]	radius of the circle
a	<input type="text"/>	[m]	wire radius
μ_r	<input type="text"/>	[]	relative permeability of the medium
L	<input type="text"/>	[H]	Inductance

Calculate

Clear

NOTE: numbers are in scientific notation (e.g.: 1.427e-9 H = 1.1427 · 10⁻⁹ H = 1.427 nH)

$$L_{circle} \approx N^2 R \mu_0 \mu_r \left[\ln \left(\frac{8R}{a} \right) - 2 \right]$$

See also notes on [Inductance Calculations](#) page.

Figure 16: Screenshot of Inductance Calculator Used

It was discovered that values yielded by the calculator were substantially larger than the actual measured values after making the inductors. This is explained by the calculator's assumption that the relative permeability of the medium is uniform throughout, which it is not. The core is constructed of Material 77 which has a

relative permeability of 2000 – 6000, depending on flux density. Therein lies the problem, much of the medium is air, which has a relative permeability of approximately 1. The disparity in the different values heavily skewed the results produced by the calculator, which was deemed unusable. What followed was largely an empirical design approach.

Originally the attempt was to make two equal inductors, however, it was later determined via testing that equal value inductors would not be able to provide sufficient voltage across the split supply. Inability to meet voltage demands with equal inductors stems largely from a combination of a poor coupling coefficient, and more so, turns ratio considerations, which are shown below:

$$\frac{V_s}{V_p} = \frac{N_s}{N_p} \quad (8)$$

where V_s is the voltage across the secondary coil, V_p is the voltage across the primary coil, and N_p and N_s are the number of turns across the primary and secondary coil respectively. By appropriate selection (1:2) of ratio of turns voltage amplification can occur and sufficient voltage can be provided. For this case N_s must be greater than N_p .

Selecting a capacitor to place in parallel with the primary inductor requires accurate characterization. Inductance measurements were performed using the Vector Network Analyzer. A Smith Chart was obtained from the Network Analyzer and the reactance at 15MHz was used to calculate the inductance. The inductance

of the primary coil that yielded optimal performance was measured to be $1.81\mu\text{H}$.

The Smith Chart produced by the Network Analyzer is shown in Figure 17.

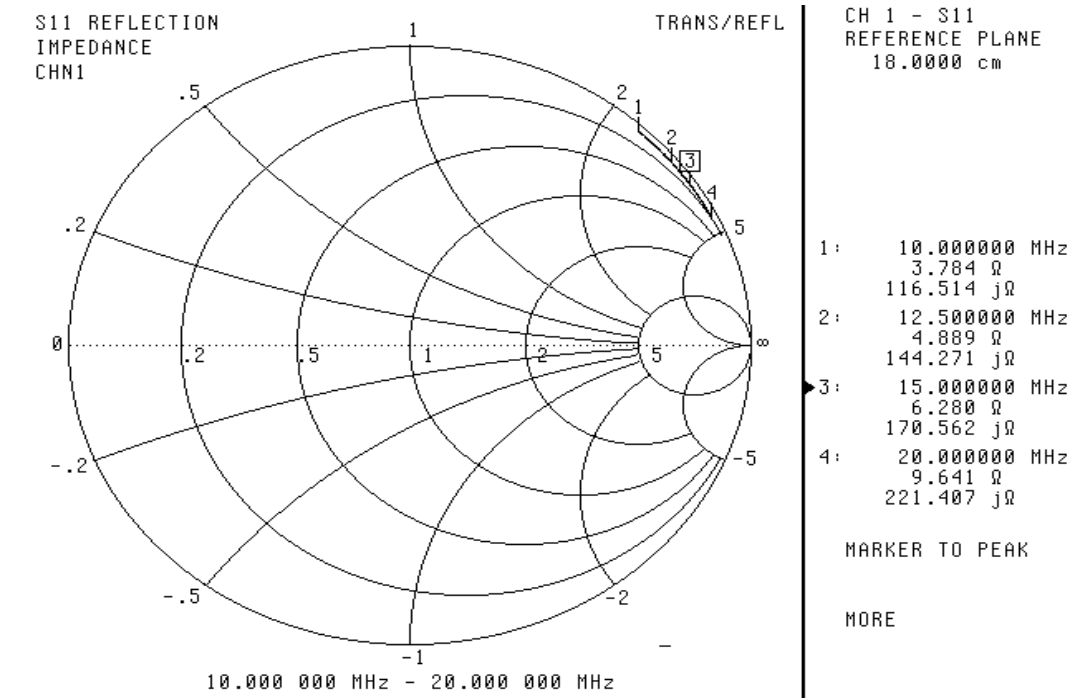


Figure 17: Smith Chart Plot of $1.81\mu\text{H}$ Primary Inductor

A capacitor value of 60pF was calculated and used for resonance at 15MHz.

A much larger inductor was used on the secondary side, measuring $6.197\mu\text{H}$.

The Network Analyzer produced Smith Chart for the secondary inductor is represented in Figure 18.

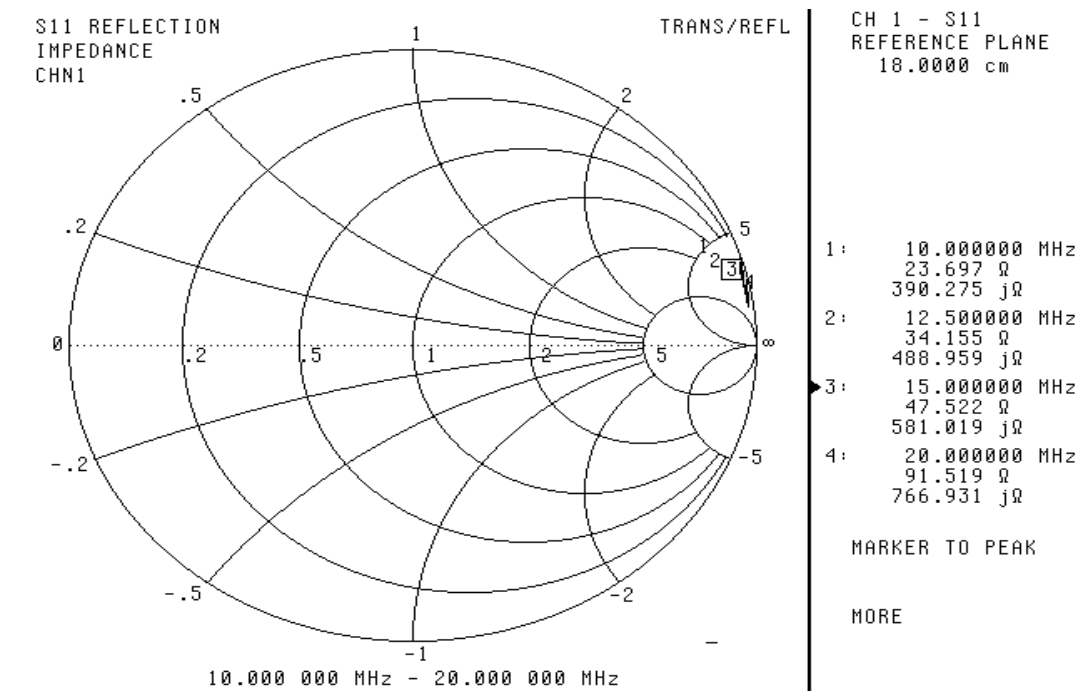


Figure 18: Smith Chart Plot of 6.197 μ H Secondary Inductor

The inductors used in the final circuit are pictured in Figure 19. The pot core height of the inductors is approximately 3mm.



Figure 19: Primary (Left) and Secondary (Right) Inductors Used in Final Circuit

During the duration of the project it was realized that the particular sensor purchased would be unable to produce measurable data without first being interfaced with a microcontroller. Using a microcontroller in the circuit was not realizable due to the increased power demands brought on by the microcontroller as well as the coding that would have been necessary for interfacing. The focus of the project shifted from a designing an actual device to instead a proof of concept demonstration. The sensor was abandoned and instead a Voltage Controlled Oscillator (VCO) was utilized to simulate data bits. The split supply was used to power the VCO and the output of the VCO connected to the control pin of the bilateral switch across the secondary coil. The VCO output is DC pulses with a selected frequency of 4kHz, similar to the output of most digital sensors. The VCO accomplishes shorting and opening of the second coil and the effects can be observed throughout the circuit.

VI. Integration and Testing

Testing had been conducted throughout to verify individual components of the system were functioning properly. Testing of the fully integrated system involved using an oscilloscope to observe the voltage across the split supply while noting the voltage required of the function generator, the effect of the switching at the both the primary and secondary coils, and the waveforms of the various output stages as they correspond to the output of the VCO. Figure 21 shows a screen capture of the oscilloscope depicting the signal across the primary coil and the voltage across the split supply.

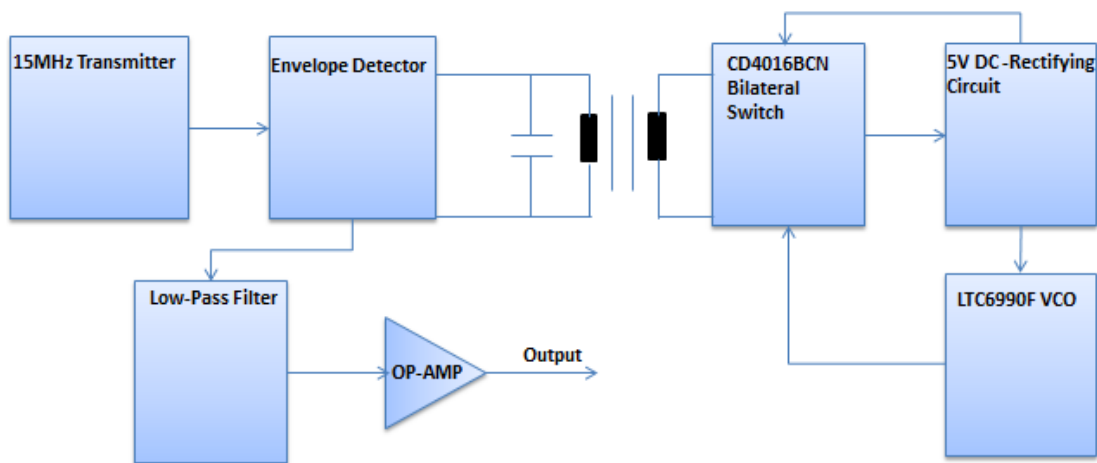


Figure 20: Functional Block System Diagram

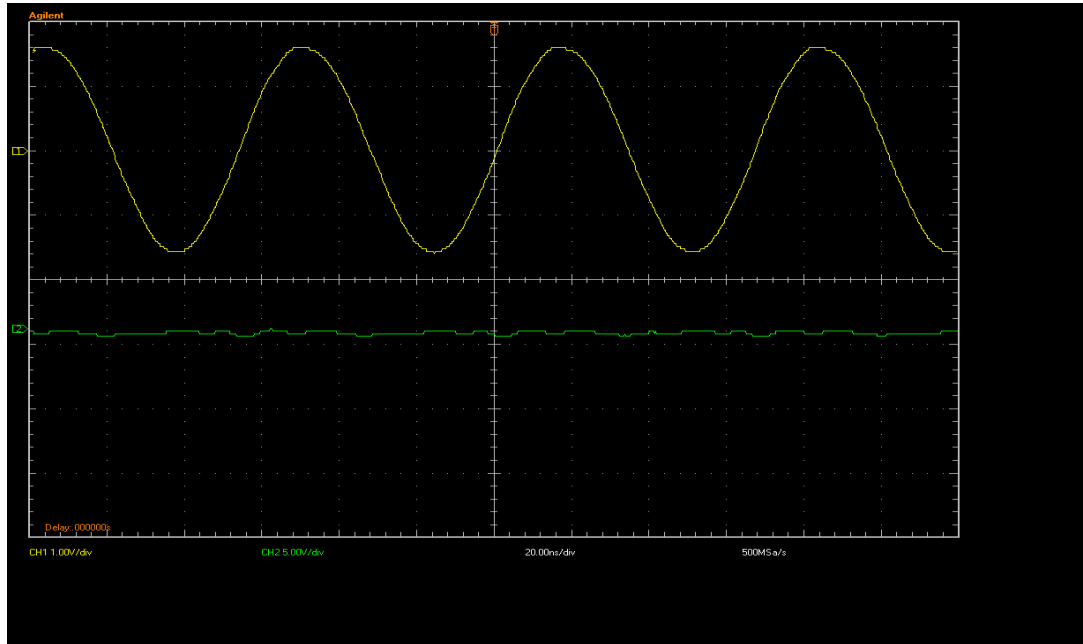


Figure 21: Channel 1 (Top) Signal Across Primary Inductor ($15V_{pp}$); Channel 2 (Bottom) 4.90V DC

A 15Vpp AC signal was supplied at a frequency of 15MHz by the Function Generator; the voltage across the primary coil shows approximately 3.2Vpp, and the voltage supplied by the split supply shows approximately 4.90V. It is important to note that the data represents measurements taken from a fully integrated and loaded system.

The envelope detector circuit designed and attached in parallel with the primary coil functioned according to theory. The output of the envelope detector showed half-wave rectification, though little can be discerned by still screen shots. The amplitude of the 15MHz signal is shown rectified and modulated, though still captures yield the 15MHz in an arbitrary state of modulation as opposed to an outline of a waveform which can be appreciated after the low-pass filter stage.

The depth of modulation is to a certain extent determined by the value of the resistor driving the circuit on the primary side, initially too small of a resistor was being used to notice significant modulation. The value of the resistor was increased to approximately 1.0k Ω , where the depth of modulation appeared to be optimized.

The low-pass filter produced a visibly modulated signal with the 15MHz carrier frequency removed. The maxima and minima of the waveform are directly related to the output of the VCO (part number LTC6990F) as shown in Figure 22.

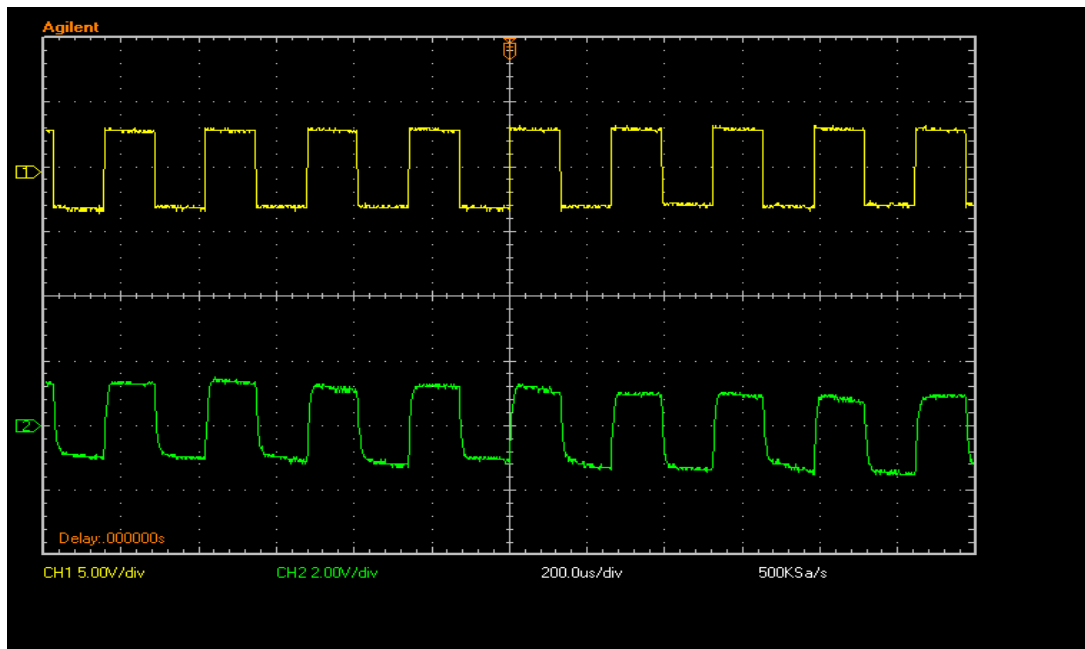


Figure 22: Channel 1 (Top) Showing the Output of the VCO ($3.3V_{pp}$); Channel 2 (Bottom) Showing the Output of Low-pass Filter ($325mV_{pp}$)

As can be seen the frequency of the modulated signal is identical to the frequency of the VCO.

In order for the data to be interpreted as logic highs and lows the signal out of the low-pass filter must be amplified. A non-inverting operational amplifier (part number LM741) was utilized; a comparator could also have been used. The resistors of the amplifier were chosen to achieve a signal with greater than 1V peak ($10k\Omega$ and $2k\Omega$ to set $V_{out} = 6V_{in}$), however, this could be further increased if necessary. A capture of the amplification stage output is shown in Figure 24.

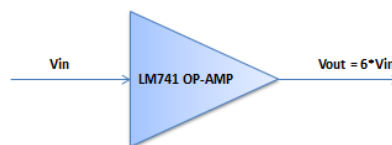


Figure 23: Showing signal amplification of 6X

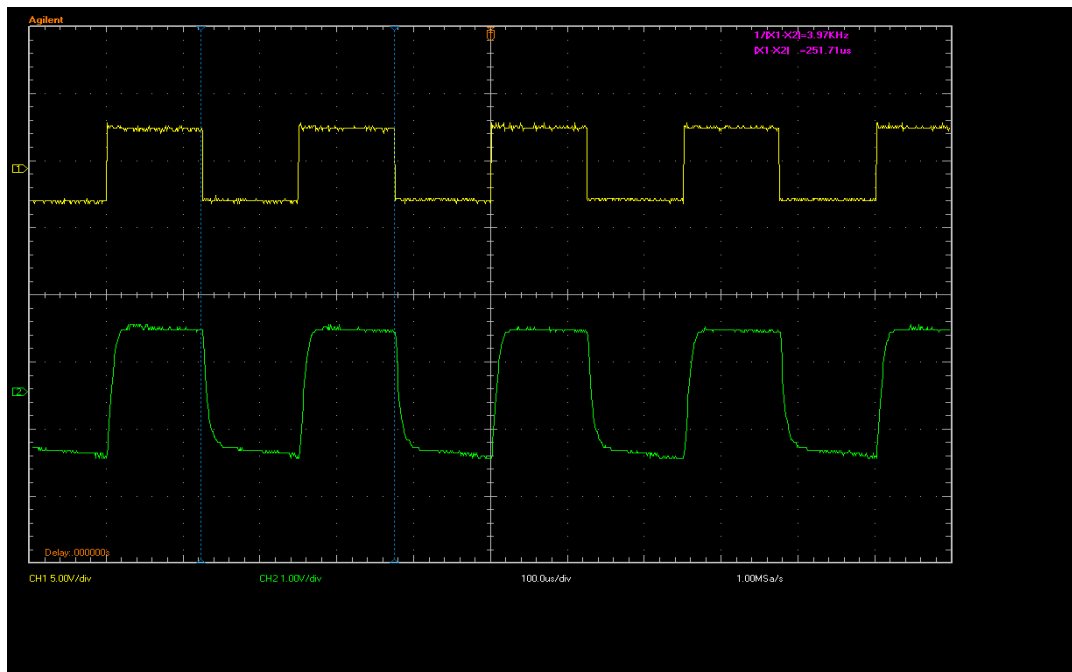


Figure 24: Channel 1 (Top) Showing the Output of the VCO ($3.3V_{pp}$); Channel 2 (Bottom) Showing the Output of the Amplification Stage ($V_{out} = 1.95V_{pp}$)

The output of the amplifier should in theory be capable of being used as an input to a microcontroller; this was beyond the scope of the project mainly due to time constraints but is an option for future research. The use of a microcontroller would enable data to be displayed on an LCD screen.

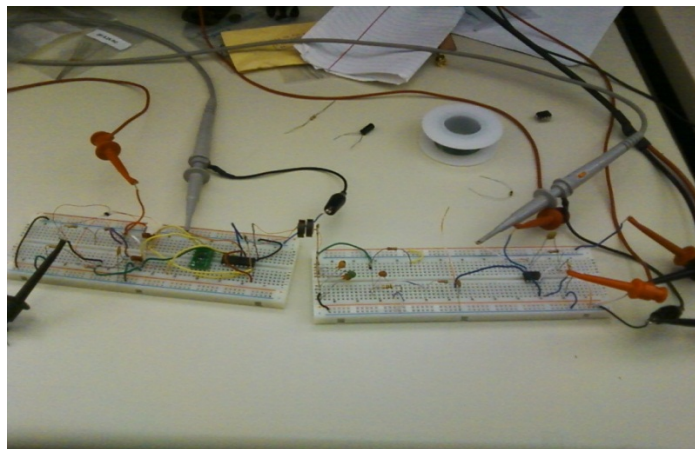


Figure 25: Final circuit prototype

VII. Conclusion and Recommendations

The design implemented in this project is capable with the use of a function generator of supplying wireless power to a passive DC pulse generator and sensing its output. The implications of such research are expansive and can be applied to numerous other fields. One such possible biomedical application would be replacing the current procedure that diabetic individuals undergo when checking blood insulin levels. Currently diabetics must puncture their finger to obtain a blood sample for analysis outside of the body. The possibility of using an implanted sensor and obtaining data wirelessly is something for consideration using the concepts presented. Another possible application would be sensing of epileptiform activity. Research being conducted on individuals suffering from epilepsy involves a permanent hole in a patient's skull increasing the patient's risk of infection as well as reducing overall protection for the brain. The initial concept of using a tire pressure sensor would still be a viable option provided a sensor better suited to this application.

One area of research that would aid advancement would be studying the effects of different media between the two coils. Having an interface of tire material between the two coils might have a consequence on the efficiency and practicality of the system. Using a higher frequency would be another topic for consideration.

The entire system prototype was constructed on two breadboards which led to a bulky and fragile circuit. The use of strictly surface mount components on a printed circuit board would dramatically reduce size and greatly improve reliability. Furthermore, using a local oscillator as opposed to a function generator would create a truly complete handheld device capable of being realized as a product.

VII. Bibliography

1. Alexander, Charles K., and Matthew N. O. Sadiku. *Fundamentals of Electric Circuits*. Boston: McGraw-Hill, 2009.
2. Iskander, Magdy F. *Electromagnetic Fields and Waves*. Englewood Cliffs, NJ: Prentice Hall, 1992.
3. Skilling, Hugh Hildreth. *Electromechanics: a First Course in Electromechanical Energy Conversion*. Huntington, NY: R.E. Krieger Pub., 1979.
4. Zverev, Anatol I. *Handbook of Filter Synthesis*. New York: Wiley, 1967.

Appendices

A. Parts List and Cost

Part	Unit Price (\$)	Quantity	Total Price (\$)
Pot Core	0.60	2	1.20
VCO (LTC6069F)	2.48	1	2.69
30-Gauge Wire	1.25	1	1.25
5082-2835 Schottky Diode	2.05	1	2.05
HSMS-2822 Schottky Diode	1.59	1	1.59
CD4016BCN Bilateral Switch	1.29	1	1.29
741 Op Amp	0.35	1	0.35
Assorted Resistors	0.10	9	0.90
Assorted Capacitors	0.50	9	4.50

Table 1: Parts List and Cost

B. Time Allocation Estimates

Task	Estimated Time (Hours)	Actual Time (Hours)
Research	35	25
Component Selection	5	15
Design	35	30
Construction/Troubleshooting	25	35
Testing	20	25
Report	25	30
Total	145	160

Table 2: Time Allocation Estimates

C. Derivation of Operating Principle

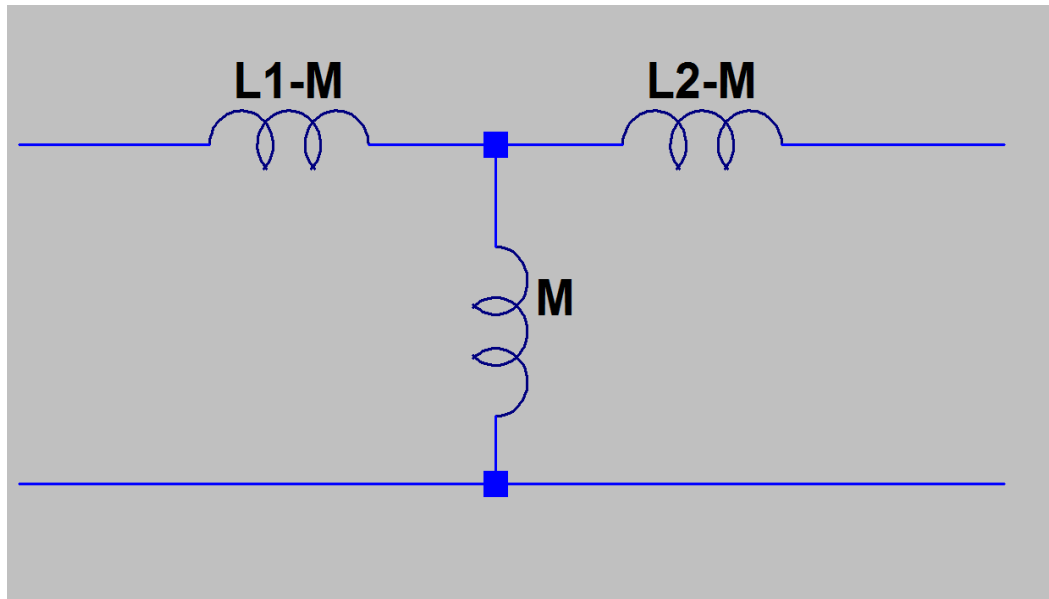


Figure 26: An Equivalent T Circuit with an Open Load

Figure 26 shows the lumped circuit equivalent of inductively coupled coils, where L_1 is the primary inductor, L_2 is the secondary inductor, and M is the mutual inductance. Applying Kirchhoff's Voltage Law produces the following equation:

$$V = I[j\omega(L_1 - M) + j\omega M]$$

which simplifies to:

$$\frac{V}{I} = j\omega L_1 - j\omega M + j\omega M$$

canceling terms and substituting $Z = \frac{V}{I}$ yields:

$$Z = j\omega L_1$$

It can be seen that input impedance of the T network when the load is left open is just the impedance of L_1 . Therefore:

$$L_{\text{seen}} = L_1$$

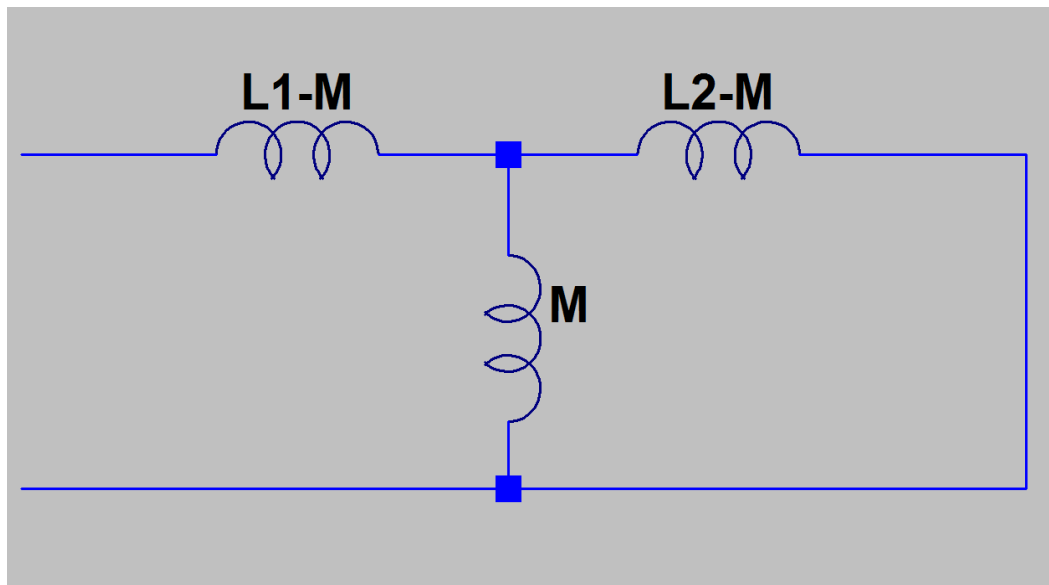


Figure 27: An Equivalent T Circuit with a Short Load

Figure 27 shows the lumped circuit equivalent of inductively coupled coils, where L_1 is the primary inductor, L_2 is the secondary inductor, and M is the mutual inductance. The case of the short load represents the case when the switch across the secondary coil is closed. Applying Kirchhoff's Voltage Law to solve for the impedance of the network produces the following equation:

$$Z = j\omega(L_1 - M) + j\omega(L_2 - M) \parallel M$$

Expanding:

$$Z = j\omega(L_1 - M) + \frac{-(L_2 - M)M\omega^2}{j\omega(L_2 - M) + j\omega M}$$

Adding terms:

$$Z = \frac{-(L_1 - M)\omega^2 L_2 - L_2 M \omega^2 + M^2 \omega^2}{j\omega L_2}$$

Expanding the numerator:

$$Z = \frac{-L_1 L_2 \omega^2 + M L_2 \omega^2 - L_2 M \omega^2 + M^2 \omega^2}{j\omega L_2}$$

Simplifying:

$$Z = \frac{M^2 \omega^2 - L_1 L_2 \omega^2}{j\omega L_2}$$

Factoring out ω :

$$Z = \frac{(M^2 - L_1 L_2)\omega}{jL_2}$$

Plugging in for $M = k\sqrt{L_1 L_2}$

$$Z = \frac{\omega(k^2 L_1 L_2 - L_1 L_2)}{jL_2}$$

Factoring the numerator:

$$Z = \frac{\omega L_1 L_2 (k^2 - 1)}{jL_2}$$

Canceling L_2 term:

$$Z = \frac{\omega L_1 (k^2 - 1)}{j} = -j\omega L_1 (k^2 - 1) = j\omega L_1 (1 - k^2)$$

$$Z = j\omega L_1 (1 - k^2)$$

Therefore, the inductance seen at port 1 when port 2 is shorted is as follows:

$$L_{\text{seen}} = L_1(1 - k^2)$$

D. Picture of Prototype

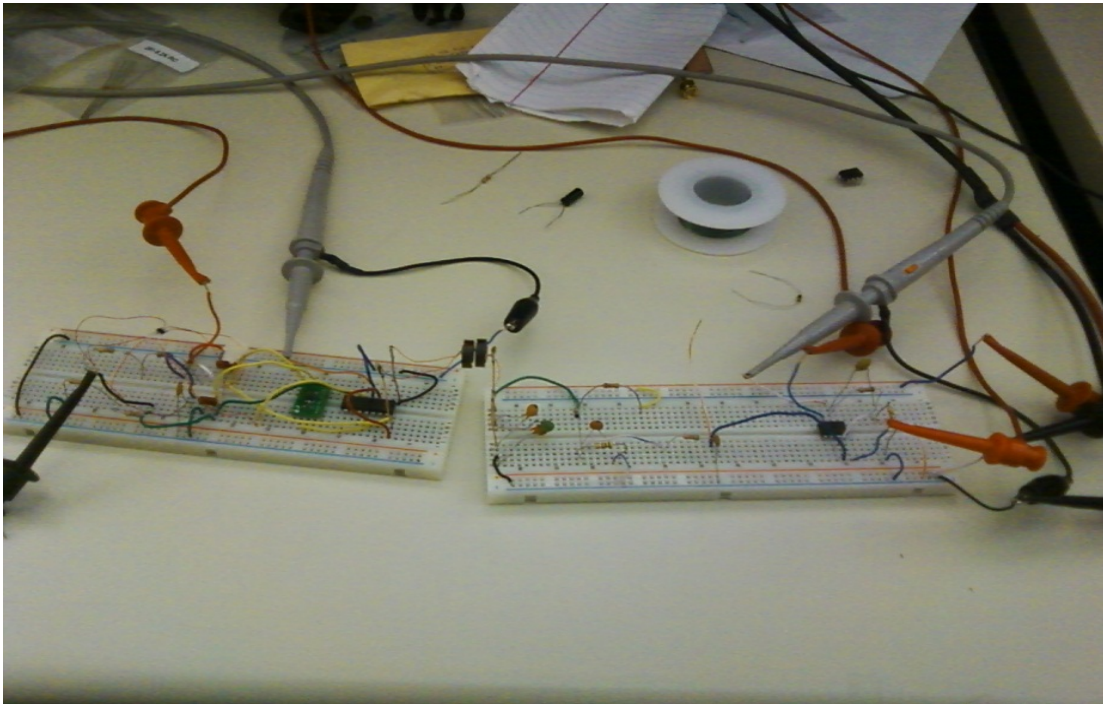


Figure 28: Picture of Prototype